Research report

Alpha-Synuclein transgenic mice, h-α-SynL62, display α-Syn aggregation and a dopaminergic phenotype reminiscent of Parkinson's disease

Silke Frahm[a], Valeria Melis[b], David Horsley[b], Janet E. Rickard[b], Gernot Riedel[b,*], Paula Fadda[d], Maria Scherma[d], Charles R. Harrington[b,c], Claude M. Wischik[b,c], Franz Theuring[a,**], Karima Schwab[a]

[a] Charité—Universitätsmedizin Berlin, Institute of Pharmacology, Hessische Str. 3-4, 10115 Berlin, Germany
[b] School of Medicine, Medical Sciences and Nutrition, University of Aberdeen, Foresterhill, Aberdeen AB25 2ZD, UK
[c] TauRx Therapeutics Ltd., Singapore 068805, Singapore
[d] University of Cagliari, Department of Neuroscience, Cittadella Universitaria, 09042 Monserrato, Italy

ARTICLE INFO

ABSTRACT

Alpha-Synuclein (α-Syn) accumulation is considered a major risk factor for the development of synucleino-pathies such as Parkinson's disease (PD) and dementia with Lewy bodies. We have generated mice over-expressing full-length human α-Syn fused to a membrane-targeting signal sequence under the control of the mouse *Thy1*-promotor. Three separate lines (L56, L58 and L62) with similar gene expression levels, but con-siderably heightened protein accumulation in L58 and L62, were established. In L62, there was widespread labelling of α-Syn immunoreactivity in brain including spinal cord, basal forebrain, cortex and striatum. Interestingly, there was no detectable α-Syn expression in dopaminergic neurones of the substantia nigra, but strong human α-Syn reactivity in glutamatergic synapses. The human α-Syn accumulated during aging and formed PK-resistant, thioflavin-binding aggregates. Mice displayed early onset bradykinesia and age progressive motor deficits. Functional alterations within the striatum were confirmed: L62 showed normal basal dopamine levels, but impaired dopamine release (upon amphetamine challenge) in the dorsal striatum measured by in vivo brain dialysis at 9 months of age. This impairment was coincident with a reduced response to amphetamine in the activity test. L62 further displayed greater sensitivity to low doses of the dopamine receptor 1 (D1) agonist SKF81297 but reacted normally to the D2 agonist quinpirole in the open field. Since accumulation of α-Syn aggregates in neurones and synapses and alterations in the dopaminergic tone are characteristics of PD, phe-notypes reported for L62 present a good opportunity to further our understanding of motor dysfunction in PD and Lewy body dementia.

1. Introduction

Parkinson's disease (PD) is the second most common neurodegen-erative disease and the most common movement disorder in humans [1,2]. The current treatments for PD are symptomatic and a disease modifying therapy is not yet available [3]. PD is characterised by the presence of intraneuronal Lewy bodies composed mainly of α-Synuclein (α-Syn) aggregates and fibrils [4]. Moreover, multiplications and mu-tations in the *SNCA* gene that encodes α-Syn are associated with

increased risk for PD [5–7]. Typically, PD is characterised by bradyki-nesia, rigidity and tremor [8] caused by dopamine (DA) depletion as a result of degeneration of dopaminergic neurones in the midbrain that have their axonal projections to the striatum, the main basal ganglia input structure [9]. Non-motor symptoms such as olfactory deficits, cognitive deficits and mood disorders represent frequent co-morbidities that may precede movement impairment [10–12].

α-Syn is highly expressed in the brain and to a lesser extent in a variety of peripheral organs [13]. It is concentrated in presynaptic

nerve terminals and involved in vesicle trafficking and release, possibly through direct or indirect interactions with the SNARE complex [4,14,15]. In disease conditions, oligomerised and aggregated α-Syn cause synaptic toxicity and neuronal degeneration [16]. During disease progression non-dopaminergic neurotransmitter systems can be affected, including cholinergic, serotonergic, GABAergic and noradrenergic driven circuitries [17,18]. Although the underlying mechanisms are yet to be defined, proposed actions for α-Syn include the promotion of oxidative stress, mitochondrial dysfunction and neuroinflammation or the disturbance of neurotransmission via its ability to interact with synaptic vesicles or the dopamine transporter [4,15,19]. Since α-Syn is believed to induce neurotoxicity and PD, several α-Syn-based mouse models have been created to capture PD-related features [20–23]. Given the high prevalence of sporadic cases of PD, innovative models that express human full length α-Syn are predicted to be more physiologically relevant. One such model is presented here.

DA imbalance in the striatum is a critical neurochemical substrate for basal ganglia dysfunction in PD [24,25]. Cortical control of the GABAergic spiny projection neurones in the striatum is modulated by DA through switching between movement promoting direct and suppressing indirect pathways. Both pathways have anatomical connectivity with the substantia nigra and express dopamine type 1 (D1) and type 2 (D2) receptors, respectively [26,27]. Loss of substantia nigra neurones depletes striatal DA and leads to a frank loss of spines and asymmetric synapses in the indirect pathway [28]. As a corollary, there is an imbalance between direct- and indirect-pathway causing the Parkinsonian movement disorder [29,30].

Here, we report a set of transgenic mouse models overexpressing full-length human α-Syn fused to a membrane-targeting signal sequence under the control of the mouse *Thy1*-promotor (h-α-Syn). Transgenic offspring from three different founder animals exhibited widespread h-α-Syn expression in cortical and subcortical regions and the degree of transgenic protein levels defined the severity of motor impairments; L62 mouse had greatest levels of α-Syn expression, which accumulated during ageing and formed PK-resistant, thioflavin-binding aggregates. Release and turnover of dopamine were impaired in aged mice (9 months), but altered responsiveness to SKF81297 was already present in young (3 months) mice despite the lack of transgene expression in dopaminergic neurones. These data re-iterate two important functional features of PD in our transgenic models and may provide a novel means for understanding the emergence and progression of striatal dysfunction in PD.

2. Materials and methods

2.1. Transgenic mice

Transgenic mice were generated by GenOway (Lyon, France). The F3.8 construct carrying a full-length h-α-Syn transgene was inserted into a pTSC21k expression vector with the *Thy1*-promotor, according to standard procedures (Fig. 1A). *Not*I linearised and purified transgenic construct was microinjected into C57BL/6J wild-type (WT) male pronucleus and fertilized oocytes were inseminated following standard procedures. Founder mice were identified by Southern blot and PCR screening from genomic DNA (forward and reverse primers were ggatctcaagccctcaaggtaaatgg and tccacgccagccagaatttatatgc, respectively; 1127 bp product) and independent homozygous transgenic lines were generated from founder animals. All behavioural experiments were conducted in accordance with the German Law for Animal Protection (Tierschutzgesetz) and the European Community Directive 63/ 2010/EU.

Male and female homozygous transgenic and WT mice were housed in small colonies in Macrolon type III (Techniplast, Brescia, Italy) cages during experimentation. Three different lines from the same DNA construct (h-α-SynL56, h-α-SynL58, h-α-SynL62 hereinafter termed L56, L58 and L62) were maintained in climatised holding rooms (20 °C
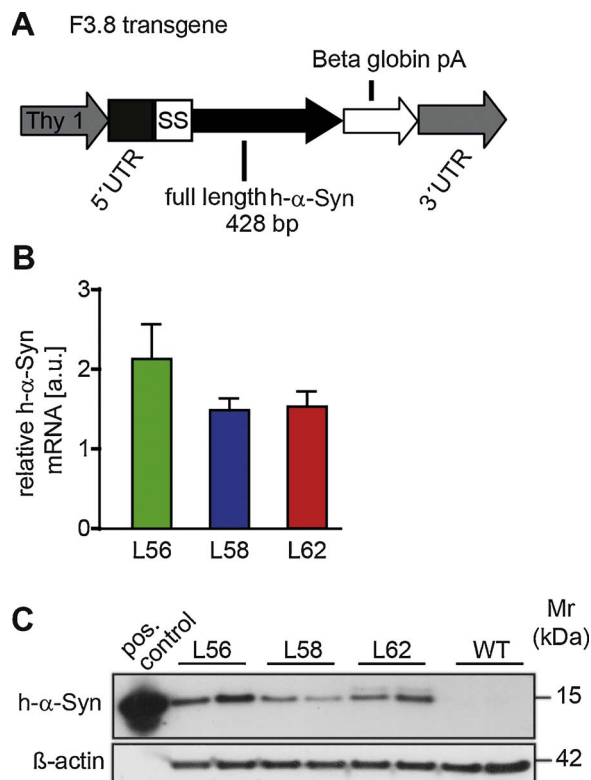

Fig. 1. Generation of transgenic mice expressing human α-Syn under the control of the mouse *Thy1*-promotor. (A) Structure of the full-length h-α-Syn construct F3.8 (428 bp) inserted into a *Thy1* expression cassette. (B) Three independent h-α-Syn transgenic lines originated from independent founder mice, named L56, L58 and L62, expressed similar levels of transgene mRNA. (C) Urea-extracted proteins from whole brain homogenate analysed by Tris-tricine SDS-PAGE and immunoblotting confirmed abundance of h-α-Syn (mAb 204) in all three transgenic lines but not in WT mice. Full-length bacterial h-α-Syn was included as a positive control.

and 40% humidity) with a 12 h light/dark cycle (lights on at 6 am) with food and water ad libitum. Details of genetic background, cohort sizes, gender distribution, age profiles, behavioural test procedure and pharmacological treatment of animals tested in each experiment are summarised in Table 1; these are not sums as some animals were tested in multiple protocols and brains were harvested from all animals. Typically, animals were derived from 3 to 4 litters and group housed immediately following weaning in cohorts of 3–6 mice separated by gender. Prior to experimentation, subjects were randomly assigned to drug groups with some limitations. Animals in each cage received the same drug and dose and were randomly tested throughout the day (9 am-4 pm with gender and transgenic line counterbalanced across the day to avoid variation). The experimenter was not blind to the condition of the animal, but histological quantifications were done by an experimenter blind to the genotype and drug condition.

From the initial characterisation, it became obvious that maximum levels of h-α-Syn positive cells were attained no later than 6 months of age. We therefore speculated that younger mice may be pre-symptomatic, especially when expressing h-α-Syn at low levels (such as L56 and 58) while cohorts aged 6 months or more could be categorised as symptomatic.

2.2. Brain tissue harvest

Mice were euthanised by cervical dislocation, the top of the skull was exposed and the overlying bone plates removed to allow harvest of the brain in an intact state. For histological analyses, brains were fixed overnight in neutral buffered formalin. For RNA measurements and urea protein extraction, whole brains were snap frozen, while for

Table 1
Cohort sizes used for behavioural and molecular assessment.

Genotype			WT			L56			L58			L62		
Age			Young	Old		Young	Old		Young	Old		Young	Old	
	Drugs	Gender	3 m	6–9 m	≥ 12 m	3 m	6–9 m	≥ 12 m	3 m	6–9 m	≥ 12 m	3 m	6–9 m	≥ 12 m
Rotarod		M + F	28	29		27	18		25	25		25	35	
Open Field/Balance beam		M + F	49	19		52	15		41	18		49	30	
CatWalk		M + F	20	30		13	30		15	29		32	29	
α-synuclein positive cell numbers in midbrain		M + F	3	3	3	27	39	45	28	42	32	26	37	69
HomeCage		M	11	10								19	21	
Elevated Plus Maze		M		25									23	
TH cell counts in SNpC		M	8	8	7							6	6	7
TH, p-TH, DAT, VMAT IB in whole brain		M		5–7	4								5–7	6
DA (including DOPAC and HVA) brain dialysis		M	10 (5)	8 (3)								9 (5)	8 (3)	
Amphetamine (AMPH)	Saline	M	9	8								10	8	
	AMPH		9	9								10	8	
SKF 81297 (SKF) and Quinpirole (QUIN)	Saline	M	8									6		
	SKF/0.5		7									7		
	SKF/5		8									8		
	QUIN		7									8		

Empty cells indicate that no measurements were performed. M = male; F = female; m = months. For details, see text.

enrichment of synaptic proteins and for thioflavin binding assays cortical tissue was dissected and snap frozen.

2.3. RNA isolation, PCR and quantitative reverse transcriptase PCR (Q-RT-PCR)

RNA was extracted from frozen whole brain tissue with the TRIzol® reagent according to the manufacturer's instructions (Invitrogen, USA) and concentration was measured using a NanoDrop 1000 spectrophotometer (ThermoFisher, USA). RNA (5 µg) was then treated with DNAse (Turbo DNA-free kit, Applied Biosystems, USA), reverse transcribed (iScript cDNA synthesis Kit, Bio-Rad, Germany) and the cDNA diluted to a final concentration of 2 ng/µL. Q-RT-PCR was carried out with Power SYBR Green (Applied Biosystems, USA). Relative mRNA expression of transgenic h-α-Syn was quantified with the ΔCt method normalized to glyceraldehyde-3-phosphate dehydrogenase (GAPDH) (h-α-Syn forward primer: caaaaccaaggagggagtg, h-α-Syn reverse primer: tcttctgggctactgctgtc, 116 bp product; GAPDH forward primer: aacgaccccttcattgac, GAPDH reverse primer: tccacgacatactcagcac, 191 bp product). Ten mice of mixed genders per line were analysed at the age of 2 months.

2.4. Protein extraction

Around 100 mg of crushed frozen whole brain tissue from 3 or 6–8 months old mice was used for preparation of urea soluble proteins. Briefly, the tissue was incubated for 45 min at room temperature in 5 vol urea buffer (7 M urea, 2 M thiourea, 70 mM DTT, 25 mM Tris/HCl, 50 mM KCl, 3 mM EDTA, 2.9 mM benzamidine and 2.1 µM leupeptin) and centrifuged at $16,000 \times g$ and RT for 45 min. The supernatant, containing urea soluble proteins, was used for analyses.

The Syn-Per Extraction Reagent (Thermo Fisher Scientific, Waltham, USA) was used to extract synaptic proteins from 6 to 8 months old mice. Briefly, 1 ml ice cold Syn-Per-Reagent was added to 100 mg crushed cortical tissue and the homogenate centrifuged for 10 min at 4 °C and $2000 \times g$ to remove cell debris. The supernatant was further centrifuged for 20 min at 4 °C and $15,000 \times g$ to obtain a cytosolic fraction (supernatant) and a crude synaptic fraction (pellet dissolved in 100 µl ice cold Syn-Per-Reagent). Both fractions were used for analyses and were either digested with proteinase K (PK) prior to immunoblotting.

For high-speed sequential extraction, the method of Brinkmann et al. (Brinkmann, MCP 2014) was used with minor modifications. Briefly, 100 µg crushed cortical tissue derived from 6 to 8 months old mice was incubated for 1 h at 4 °C in 500 µl 10 mM tris buffer (homogenate fraction H), and centrifuged for 1 h at 4 °C and $100,000 \times g$ to produce a supernatant (S1) and a pellet fraction. The pellet was solved in 450 µl 10 mM tris-0.5% Triton-X-100, incubated for 1 h at 4 °C and thereafter centrifuged for 1 h at 4 °C and $100,000 \times g$ to produce a supernatant (S2) and a pellet fraction. The latter was again incubated for 1 h at 4 °C in 450 µl 10 mM tris-2% Triton-X-100 and centrifuged for 1 h at 4 °C and $100,000 \times g$. The supernatant fraction S3 was retained and the pellet fraction was incubated for 1 h at 12 °C in 450 µl 10 mM tris-0.5% SDS and centrifuged for 1 h at 12 °C and $100,000 \times g$. The resulting supernatant S4 was retained and the final pellet solved in one volume 10 mM tris-0.5% SDS. All fractions were stored at −20 °C.

2.5. Protein K cleavage

Synaptic or cytosolic proteins (50 µg) were mixed with or without 1 µl PK (diluted 1:1000 in PBS, stock concentration of the enzyme was 20 µg/µl), incubated for 15 min at 37 °C and the reaction was stopped by cooling down on ice.

2.6. Immunoblotting

For immunoblotting of urea soluble proteins, 25-µg protein extracts were loaded on 10% Tricine-SDS-PAGE. The cathode buffer consisted of 100 mM Tris, 100 mM Tricine and 1% (w/v) SDS and the anode buffer contained 100 mM Tris and 0.07% (v/v) HCl. Following electrophoresis, proteins were transferred to PVDF membranes by semi-dry blotting in 300 mM Tris, 6% (v/v) acetic acid at 4 °C following standard procedures [31]. Membranes were incubated with primary antibodies against h-α-Syn (mAb 204 from Santa Cruz Biotechnology, diluted 1:200), tyrosine hydroxylase (TH, H-196 from Santa Cruz Biotechnology; diluted 1:1000), vesicular monoamine transporter 2 (VMAT2, C-20 from Santa Cruz Biotechnology; diluted 1:500), dopamine transporter (DAT) (AB1591 from MerckMillipore; diluted 1:500) and phospho-serine 40 TH (#2791 from Cell Signaling Technology USA; diluted 1:1000). Immunoblots were washed three times in PBS, incubated in horseradish peroxidase-conjugated secondary antibodies diluted 1:5000 (Dako, Denmark), washed again three times in PBS and developed by chemiluminescence (GE Healthcare, USA). Human α-Syn was measured in 3 months old mice, pSer40-TH, DAT and VMAT2 in

6–8 old mice and TH in 6–8 and 12 month old mice. Primary and secondary antibodies were diluted in 4% (w/v) BSA-TBS containing 0.2% (v/v) Tween-20.

For immunoblotting of synaptic and cytosolic proteins, 25-μg protein pre-treated with PK was loaded on 10% Tricine-SDS-PAGE and transferred to PVDF membranes after electrophoresis. Membranes were incubated with primary antibodies against h-α-Syn (mAb 204) or ß-tubulin (#15115 from Cell Signaling Technology USA; diluted 1:5000) and immunoblots were developed by chemiluminescence as described above, after applying appropriate secondary antibodies.

2.7. Thioflavin binding assay

The binding assay was conducted in 96-well plates using the six fractions derived from the sequential extraction described above. Briefly, 50 μg protein extracts from each of the six fractions were incubated with 100 μl aqueous Thioflavin T solution (10 μM) at RT in the dark. The plate was covered with a lid and was well sealed with parafilm to avoid any volume change through evaporation and the fluorescence was measured after 4 h, 1, 2, 3, 4, 7 and 8 days. The excitation wavelength was set to 485 nm, while the emmission signal was measured at 460 nm. Each sample was measured in duplicates.

2.8. Immunohistochemistry and cell counting

Formalin-fixed and paraffin-embedded brain tissue was cut into 5-μm thin coronal sections. For staining using peroxidase-based detection, sections were deparaffinised, boiled in 10 mM citric buffer for antigen retrieval and incubated in 0.3% (v/v) hydrogen peroxidase solution. Sections were blocked for 20 min in blocking buffer (0.1% (w/v) BSA in PBS), incubated in primary antibody diluted in blocking buffer for 1 h at RT, followed by incubation with corresponding biotinylated secondary antibody diluted 1:100 in blocking buffer (Dako, Denmark). Anti-h-α-Syn (mAb 204 from Santa Cruz Biotechnology (USA), diluted 1:100) and anti-TH (H-196 from Santa Cruz Biotechnology, diluted 1:100) were used. Sections were developed with diaminobenzidine solution (Dako, Denmark), counterstained with Ehrlich haematoxylin solution (Carl Roth, Germany), embedded in Neo-Mount® (Merck Millipore, Germany) and images taken using a light microscope (Carl Zeiss, Jena, Germany).

For immunofluorescence, sections were deparaffinised, boiled in 10 mM citric buffer, blocked for 1 h in incubation buffer (5% (v/v) normal goat serum in PBS containing 0.3% (v/v) Triton-X-100) and incubated in primary antibody cocktails (mAb 204/TH; mAb 204/DAT; mAb 204/synaptophysin or mAb 204/VGLUT1). Primary antibodies against h-α-Syn (mAb 204 from Santa Cruz Biotechnology, diluted 1:100), TH (H-196 from Santa Cruz Biotechnology diluted 1:100), DAT (AB1591P from Merck-Millipore (USA), diluted 1:500), synaptophysin (#101002 from Synaptic Systems (Germany), diluted 1:1000) and VGLUT1 (#135302 from Synaptic Systems, diluted 1:1000) were all diluted in incubation buffer and were applied overnight at 4 °C. The next day sections were incubated for 1.5 h in fluorochrome-conjugated secondary antibodies (Alexa Fluor® 488-conjugated donkey anti-mouse IgG and Alexa Fluor® 568-conjugated goat anti-rabbit IgG, Life Technologies, USA; both diluted 1:500 in incubation buffer), covered with DAPI Gold Antifade Reagent (Cell Signaling Technology, MA, USA) and examined using a microscope equipped for fluorescence (Carl Zeiss, Germany). Counting of h-α-Syn-positive or TH-positive neurones was performed manually for 3 consecutive brain sections at positions relative to Bregma, as identified according to [32], and the mean value for each animal was used in analyses. Cells immunoreactive for h-α-Syn were counted for one entire brain hemisphere at Bregma +3.80 ± 0.25 mm. TH-positive dopaminergic neurones were identified in substantia nigra pars compacta (SNpC) at Bregma −3.80 ± 0.25 mm.

2.9. In vivo brain microdialysis

In general, the procedure established in Fadda et al., was applied [33]. Mice were anaesthetised with Equithesin (0.52 ml/kg i.p.), placed in a stereotaxic frame (David Kopf Instruments, Tujunga, CA) with the skull horizontal, and small burr holes drilled unilaterally to harbour the chronically implanted 2-mm long concentric microdialysis probe (AN 69AF, Hospal-Dasco, Italy, cut-off 40,000 kDa) at coordinates Bregma AP + 1.2, L ± 1.5, V-3.5 [32] to extend into the dorsal striatum. The probe was anchored to the skull with acrylic cement and mice were allowed to recover for at least 24 h. For microdialysis, artificial cerebrospinal fluid (CSF: 147 mM NaCl, 4 mM KCl, 1.5 mM CaCl$_2$, pH 6-6.5) was circulated through the probe at 2.5 μl/min and 50-μL samples were collected every 20 min. Dopamine and metabolites were separated by HPLC (ESA Coulochem II detector) with electrodes band pass filtering between +400 mV (low-pass) and −180 mV (high pass) at 30 °C. The mobile phase consisted of 50 mM sodium acetate, 0.073 mM Na$_2$EDTA, 0.35 mM octenylsuccinic anhydride, 12% methanol, pH 4.21, flow rate 1.0 ml/min). Dopamine and its metabolites 3,4-dihydroxyphenylacetic acid (DOPAC) and homovanillic acid (HVA) were measured.

2.10. Behavioural phenotyping

2.10.1. Open field test with and without drug treatment

The open field arena consisted of a 120 × 120 cm large grey Perspex square with 40-cm high walls, placed 75 cm above the ground and surrounding cues obscured by white curtains. Mice were released in the centre of the arena and allowed to move freely for up to 30 min. Ambulatory movement of the animals was recorded by an overhead CCTV camera and the path of the animal recorded at 12 Hz was video tracked and stored online as XY coordinates using EthoVision XT10 (Noldus IT, Wageningen, The Netherlands). From these coordinates, we extracted the overall activity (distance moved) in each session.

For pharmacological studies, mice were placed in the centre of the arena immediately after intraperitoneal injection of saline or drug and locomotor activity was recorded for 30 min. Dugs included: 2 mg/kg d-amphetamine sulphate (Lipomed, Weil am Rhein, Germany); 0.5 or 5 mg/kg of D1 agonist (±)-6-Chloro-2,3,4,5-tetrahydro-1-phenyl-1*H*-3-benzazepine hydrobromide (SKF81297 from Tocris); 0.025 mg/kg of D2 agonist quinpirole hydrochloride (Sigma-Aldrich, Gillingham, UK). Since preliminary experiments with SKF81297 revealed that the behavioural effect starts approximately 20 min after injection, the duration of the experiment was prolonged to 60 min, according to the pharmacokinetic profile of the drug.

2.10.2. Home cage activity monitoring (conducted at the Berlin Mouse Clinic for Neurology and Psychiatry, Berlin, Germany)

Male mice, aged 3 and 6 months, were anaesthetised with 1–3% isoflurane and tagged subcutaneously with individual radio-frequency-identification (RFID) transponders (planet-ID GmbH, Germany). Mice were housed 4–6 per cage (type II-L) and allowed to acclimatise to the testing room for one week. Cages were placed onto an RFID sensor plate consisting of 2 × 4 RFID sensors positioned in a grid-like formation (Activity Monitor, PhenoSys, Berlin, Germany). This apparatus identifies the unique RFID tag of each mouse and tracks position and movement over time (sampling rate 3 Hz). The X and Y coordinates were continuously recorded for 48 h (weekend days, to avoid the presence of the experimenter) and written directly in csv format to the hard drive of a PC. Values were extracted for each mouse individually in hourly bins, pooled for day-night cycle and are presented as a mean distance travelled during light and dark phase.

2.10.3. RotaRod

A 4-lane RotaRod system for rats was used (33700-R/A; Technical & Scientific Equipment GmbH, Bad Homburg, Germany). Animals were given a single trial of 10 min with a constant velocity of 6 rotations per

minute (rpm). Mice were placed onto the rod at an initial speed of 1 rpm and the speed accelerated to maximum over 30 s. The trial was ended when the animal fell off the rod or after 10 min and the time sustained was noted as the dependent variable.

2.10.4. Gait analysis

A detailed analysis of the walking pattern of mice was performed using the CatWalk (Noldus IT). The apparatus consisted of a 45×10 cm glass plate illuminated by a laterally positioned light source. A camera was mounted to the underside of the glass plate to observe footfalls as a change in brightness. Animals were released at one end of the runway and 5 runs across the plate were monitored. Data were recorded, stored and analysed using the Catwalk XT9 software (Noldus IT). Numerous gait parameters were analysed including base of support, swing, and regularity index (for details, see [34]).

2.10.5. Balance beam

The experiment was performed as described previously [35]. In brief, 50-cm long wooden beams were positioned at an angle of 30° inclination. Beams were square or round with a diameter of 28, 11 and 5 mm; a trial lasted up to 30 s and no prior training was administered. The time to traverse the beam was recorded. If animals did not reach the top end of the beam, the maximum time of 30 s was noted.

2.10.6. Elevated plus maze

The maze made of grey Perspex was placed 75 cm above the ground and consisted of four arms, each 30 cm long and 5 cm wide, with two open arms without walls and two enclosed arms surround by 15 cm high walls. Mice were released in the centre of the maze and were allowed to move freely for up to 10 min. The movement of the animals was recorded by an overhead CCTV camera connected to a PC running EthoVision XT10 (Noldus IT). XY coordinates of the animal were tracked at a sampling rate of 12 Hz and converted into time spent in the open versus enclosed arms.

2.11. Data analyses

Histological quantifications and behavioural data were expressed as group mean (and standard error of the mean, S.E.M.). Statistical analyses were conducted using GraphPad Prism (version 6.00; GraphPad Software Inc., La Jolla, CA, USA), confirmed as Gaussian (D'Agostino and Pearson omnibus test) and analysed by parametric statistics (unless stated otherwise) using factorial analysis of variance (ANOVA) and appropriate post-hoc (t-test; Bonferroni corrected) two-tailed tests (for details, see Results). The null hypothesis was accepted for $\alpha < 0.05$ and only significant terms are given in the text.

3. Results

3.1. Generation of transgenic mice and h-α-Syn expression

Transgenic mice were generated by overexpressing full-length human α-Syn fused to a membrane-targeting signal sequence under the control of the mouse *Thy1*-promotor. Pronuclear injection of the construct (Fig. 1A) resulted in 3 founders expressing the transgene. Founder mice were back-crossed with C57BL/6J wild-type mice, the colony expanded and homozygous independent transgenic lines L56, L58 and L62 generated. Mice from all transgenic lines presented in good health throughout the life span, and showed normal germline transmission and mortality rates (data not shown). As depicted in Fig. 1B, similar levels of h-α-Syn mRNA were expressed in all three lines (F < 1.6). Furthermore, SDS-PAGE and immunoblotting revealed a single specific h-α-Syn band at 15 kDa (Fig. 1C). Immunohistochemical analysis confirmed neuronal localisation of h-α-Syn immunoreactivity in all transgenic lines (Fig. 2A) but not in WT mice. As expected for the *Thy1*-promotor, a widespread distribution of α-Syn was observed,

including hippocampus, dentate gyrus, cortex, entorhinal cortex, substantia nigra pars reticulata (SNpR), olfactory bulb and spinal cord (Fig. 2B). Comparative counting of cells in one hemisphere of 3 averaged coronal midbrain sections (Bregma -3.80 ± 0.25 mm) using the monoclonal antibody mAb 204 showed a low level of h-α-Syn accumulation in the brain of L56 mice at 3 months, which increased progressively from 6 to 12 months (F(2,104) = 24.58, $p < 0.0001$ for main effect of age, Fig. 2C, see asterisks for post-hoc Bonferroni test;). By comparison, L58 mice displayed moderate numbers of h-α-Syn inclusions and the number of midbrain neurones positive for h-α-Syn did not progress with ageing (Fig. 2C). The greatest level of h-α-Syn labelling was observed in L62 in both cortical and subcortical regions (Fig. 2B, a–d), but also in the olfactory bulb and spinal cord (Fig. 2B, e and f). Intense labelling was evident in both cell bodies and dendrites and, in tissue from older L62 mice, granular inclusions in cortical neurones were observed (not shown). The greatest number of α-Syn-positive cells was observed at 3 months whereas a significant decline occurred between 6 and 12 months (F(3,227) = 11.00, $p < 0.0001$ for main effect of age; see Fig. 2C for Bonferroni post-hoc tests) suggesting neuronal loss.

3.2. Sensory-motor deficits are present in high-expressing h-α-Syn mice (L58, L62)

Movement-related phenotypes were determined in a series of tests on the three h-α-Syn lines at different ages. Tests included the rotating rod with constant speed to determine the emergence of fatigue; the open field for the assessment of movement initiation and ambulatory activity; the CatWalk system for gait parameters; and the balance beam task for sensory-motor coordination.

For the open field, normality of the data set was confirmed and subtle differences were observed (Fig. 3A). At 3–4 months, all animals walked for an average of 180–200 m during 30 min. The overall ANOVA confirmed a genotype difference (F(3,187) = 5.9; $p = 0.0008$) with significantly reduced ambulation in L62 relative to control (Fig. 3A left panel asterisk). This phenotype became more severe in older L62 subjects (F(3,78) = 8.1; $p < 0.0001$) and also emerged in L58 (Fig. 3A, right panel, asterisks for Bonferroni corrected t-test).

Data were skewed for the RotaRod since a considerable number of mice were able to stay on the rod for the maximum 10-min period. Consequently, data were not normally distributed and were analysed using Kruskal-Wallis followed by Dunn's multiple comparison test. Although we detected some differences in sustaining balance and progressively walking forward in the different genotypes at 3–4 months (Fig. 3B; H = 15.1; $p = 0.002$), this was due to differences between the three genotypes, rather than a difference from WT. At 6–8 months of age, there was an overall difference (H = 23.2; $p < 0.0001$), with L58 reliably outperforming WT mice (Fig. 3B, asterisks).

Although several gait parameters were analysed from the CatWalk, only the stride length of the fore paws was affected by transgene expression (Fig. 3C). At 3–4 months, no reliable difference between controls and transgenic lines were observed although the overall ANOVA returned s significant term between group (F(3,76) p = 0.028). At 6–8 months, however, the overall difference between groups was significant (F(3,114) = 10.2; p < 0.0001) confirming longer fore paw strides in lines 56 and 62 (see asterisk in right panel for Bonferroni corrected t-test).

In the balance beam coordination task, apart from the expected main effect of beams (Fig. 4A, $F_{beam}(5,1090) = 194.4$; $p < 0.0001$), highly significant genotype differences emerged (Fig. 4A, $F_{genotype}(3,208) = 20.6$; $p < 0.0001$). L56 and L58 mice, aged 3–4 months, were outperforming WT control litters in all beams tested, including square-shaped and round beams (Fig. 4A asterisk for Bonferroni corrected t-tests), while no differences were seen between L62 and WT mice. At 6–8 months of age genotype related differences emerged only for L62 compared to WT control mice (Fig. 4B,
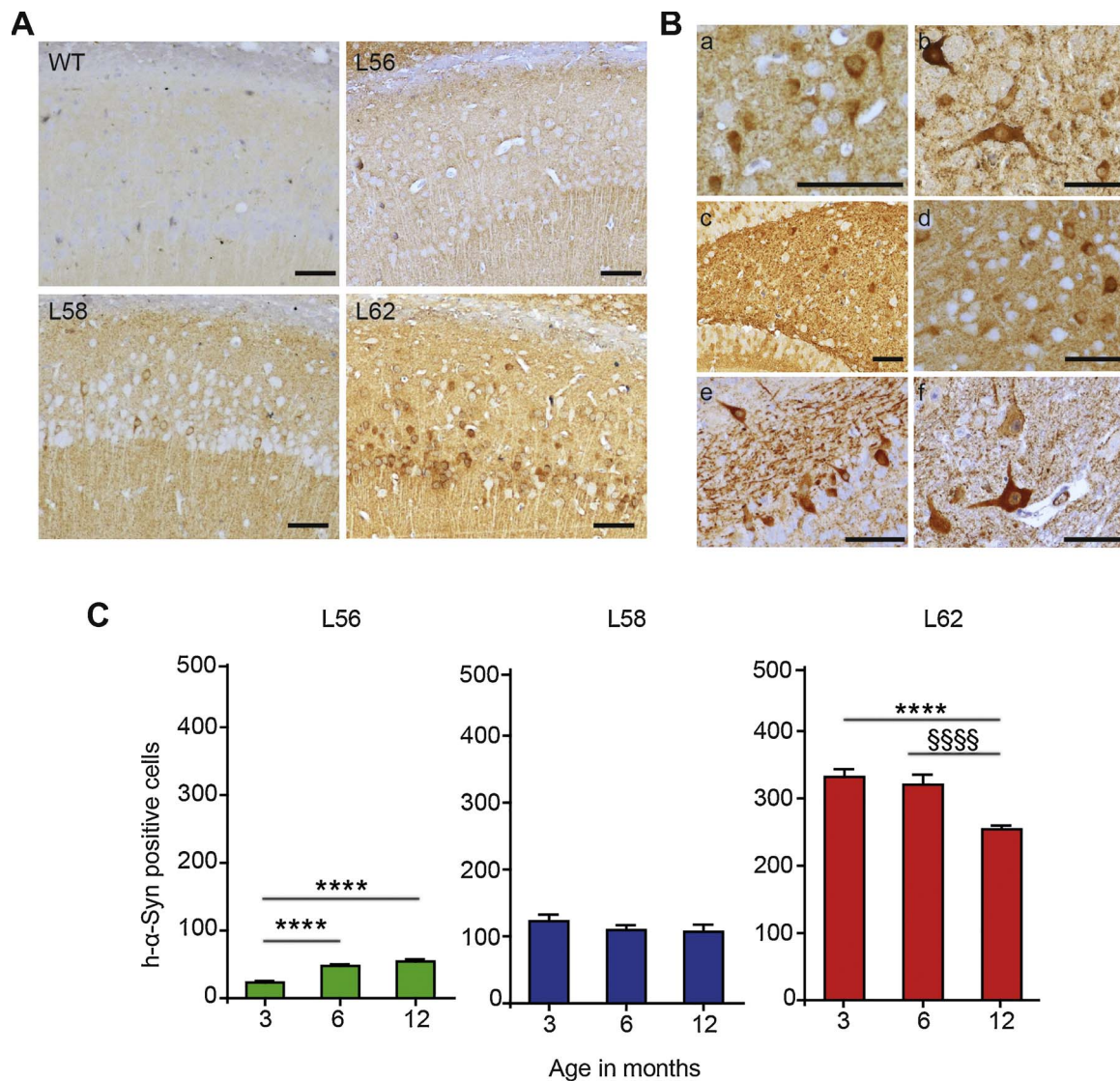
Fig. 2. Transgenic h-α-Syn is highly abundant and widely distributed in L62 mouse brain. (A) Human α-Syn immunohistochemistry (mAb 204) in midbrain sections of WT, L56, L58 and L62 revealed abundant expression of h-α-Syn in transgenic mice only, as shown by representative micrographs of the hippocampus. (B) In L62, h-α-Syn inclusions were present in different brain areas such as cortex (a), SNpR (b), dentate gyrus (c), entorhinal cortex (d), olfactory bulb (e) and in spinal cord (f). (C) Quantification of h-α-Syn positive cells (mAb 204) counted in one hemisphere of 3 averaged coronal midbrain sections at Bregma level -3.80 ± 0.25 mm for the three different transgenic lines. L62 shows the greatest number of cells expressing the transgene and an age-dependent decrease in protein expression. Values are given as mean $\pm$ S.E. Bonferroni post-test: *: $p < 0.05$ and ****: $p < 0.0001$ vs. 3 months, §§§§: $p < 0.0001$ vs. 6 months. Scale bars, 100 μm.

$F_{genotype}(3,91) = 3.7$; $p < 0.0001$), where L62 mice needed significantly more time to climb the 5 mm square-shaped and 5 mm round beams (Fig. 4B asterisk for Bonferroni corrected t-test).

Since mice of L62 appeared to be most affected in their voluntary movement by the expression of high levels of h-α-Syn, we profiled their activity in the social environment of the home cage (Fig. 5). Also, given that we did not observe a gender bias in any of our previous data sets, the further in-depth analysis concentrated on male mice. The long-term recording for each mouse was extracted; the values averaged for each genotype and plotted over a 24-h cycle. Cohorts showed typical circadian rhythms with heightened nocturnal ambulatory activity and predominant sleep/quiescence during the day. Globally, young males were more active and covered greater distances than old males during the activity period (compare ordinate of Fig. 5A and B) and it was evident that L62 mice were hypoactive during the night relative to controls (genotype F(1,31) = 16.1., $p = 0.0003$ for young and F(1,38) = 10.69, $p = 0.0023$ for old male subjects). This was particularly obvious during the beginning and the end of the night phase (interaction between genotype and time: F(23,713) = 12.59, $p < 0.0001$ for young and F

(23,874) = 6.68, $p < 0.0001$ for old males; see asterisks in Fig. 5A and B). From this activity pattern, it is apparent that male WT mice follow the pattern that is typical for C57BL/6J males, i.e. there was an activity peak during the early and late hours of the dark phase, respectively [36,37]. These activity peaks are strongly reduced in L62 mice. No differences were observed during the light phase.

Anxiety-related behaviours in the elevated plus maze (Fig. 5C–F) revealed comparable performances between L62 and WT mice, as shown for the time spent in open arms (Fig5C), time spent in centre (Fig. 5D), number of entries into open arms (Fig. 5E) and total distance moved (Fig. 5F).

The hypoactivity phenotype seen for L62 mice during the examinations in the open field and the home cage, as well as the normal anxiety phenotype in the elevated plus maze strongly suggest that the impairment in the motor activity in this transgenic line is not related to novelty or stress-induced anxiety. Collectively, it appears that increased levels of h-α-Syn lead to more severe impairments in motor activity and coordination. As L62 presented with the most widespread h-α-Syn pathology and most prominent motor phenotype compared to L56 and
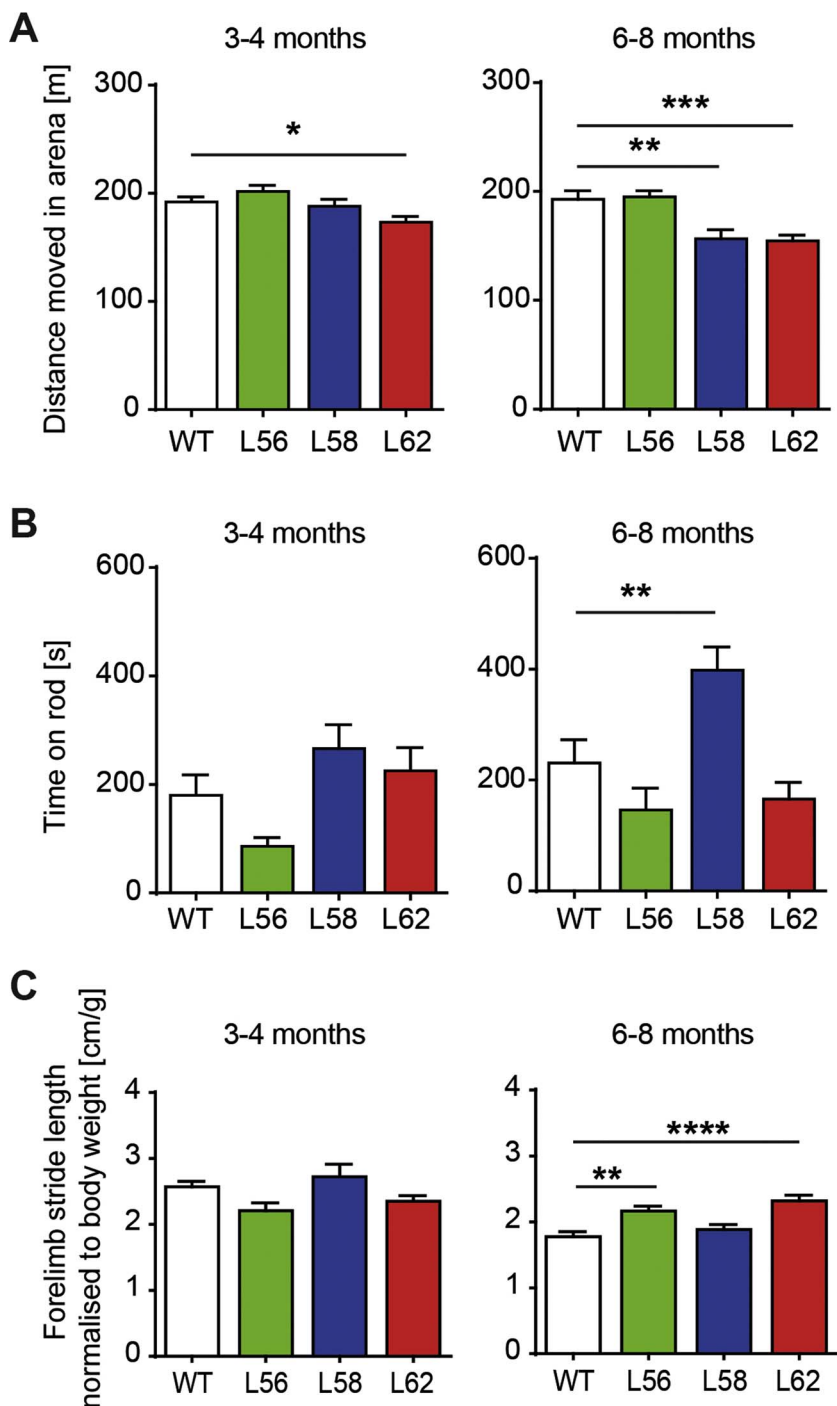
Fig. 3. Early-onset and age progressive motor deficits in L62 mice. (A) L62 walked less in the open field compared to WT at 3 months of age and this phenotype became more severe in older subjects and was also observed in L58. (B) The motor coordination measured as time spent on a rotating rod was improved in L58 mice compared to WT at 6 months of age. (C) Furthermore, L58 and L62 mice showed deficits in motor coordination, as measured by the stride length in the CatWalk. Values are given as mean $\pm$ S.E of stride corrected for weight. Dunns multiple comparison post-test for non-Gaussian data sets was used in (B), all other data were applied to Bonferroni post-test: *: $p < 0.05$, **: $p < 0.01$, ***: $p < 0.001$ vs. WT.

L58, the following functional analysis concentrated on this line.

3.3. Transgenic h-α-Syn is absent in dopaminergic but present in glutamatergic synapses

To identify neuronal populations affected by h-α-Syn pathology, immunofluorescence double labelling was performed in L62 brain sections. The antibody mAb 204 for h-α-Syn was applied with either TH (H-20) or DAT for dopaminergic neurones or VGLUT1 (#135302) for glutamatergic neurones. Transgenic h-α-Syn was absent from TH-positive dopaminergic neurones of the SNpC and nigrostriatal projections of the medial forebrain bundle, as well as from catecholaminergic neurones of the locus coeruleus (Fig. 6A for h-SynL62 and Supplementary Fig. 1A for h-SynL56/h-SynL58). H-α-Syn also did not co-localise with

DAT-positive dopaminergic terminals in the striatum (Fig. 6B), but h-α-Syn was strongly expressed in synapses, e.g. motor cortex and striatum, and h-α-Syn immunoreactivity clearly co-localised with the synaptic marker synaptophysin (Fig. 6C). These synapses harbouring h-α-Syn are glutamatergic as confirmed by co-staining with VGLUT1 (Fig. 6D).

3.4. Transgenic h-α-Syn accumulates during ageing, is resistant to PK-cleavage and binds thioflavin

While the number of neurones with h-α-Syn inclusions in L62 mice declined during ageing (Fig. 2C), a very prominent increase of h-α-syn immunoreactivity was observed e.g. in cell bodies and nerve terminals of the motor cortex (Fig. 7A) and in striatal terminals (Fig. 7B) of old animals, suggesting an age dependent accumulation of the transgenic
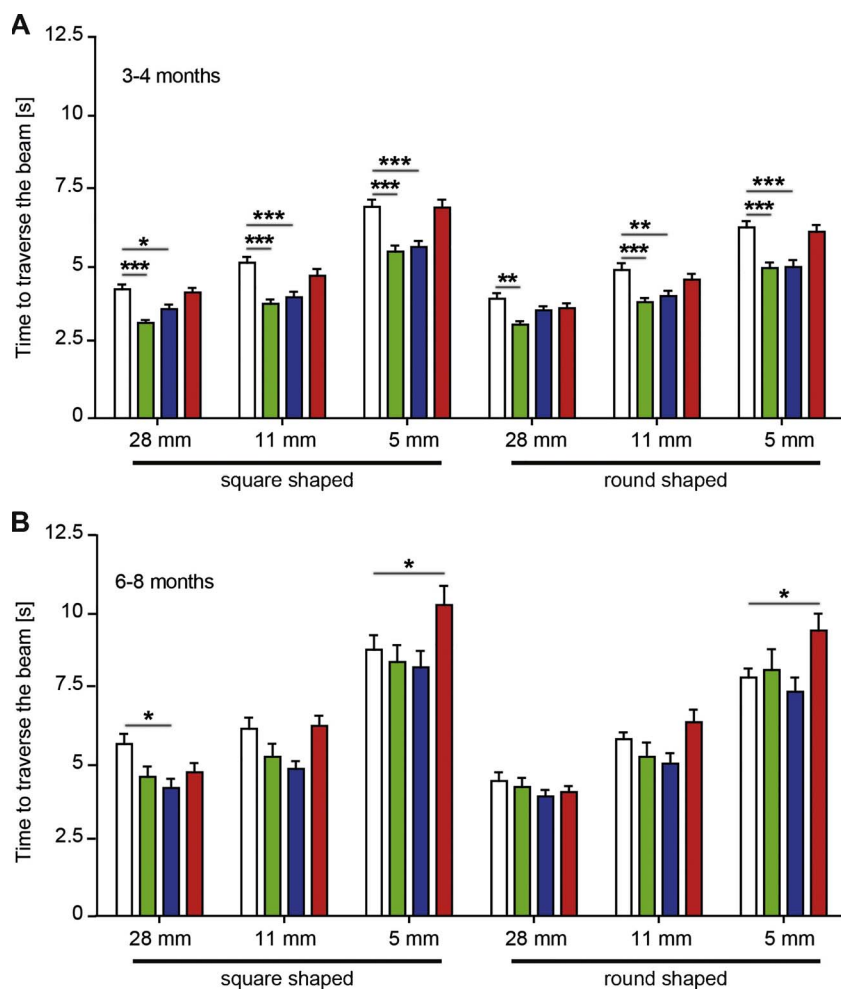
Fig. 4. Reduced motor coordination in L62 mice in the balance beam task. Age dependent performance in the balance beam test of WT, L56, L58 and L62 and mice at 3–4 (A) and 6–8 (B) months on 28-, 11- and 5-mm square-shaped and round beams, revealed improved motor coordination in 3–4 months old L56 and L58 mice as compared to WT litters, while a reduced motor coordination was observed for 6–8 months old L62 mice on the 5-mm beans (square-shaped and round beams). Values are given as mean ± S.E. Bonferroni post-test: *: $p < 0.05$, **: $p < 0.01$, ***: $p < 0.001$ vs. WT.

protein. Having established the presynaptic localisation of α-syn in the motor cortex and striatum (Fig. 6C), crude synaptic fractions were prepared from cortical lysates and digested with PK. Immunoblot analysis revealed that h-α-syn is more abundant in synaptic compared to cytosolic fractions of L62 mice and that h-α-syn per se is resistant to enzymatic cleavage with PK, while ß-tubulin is not (Fig. 7C and D). When cortical tissue was subjected to sequential high-speed extraction using detergent and Thioflavin-binding was performed, it became obvious that an increased signal of Thioflavin is seen in transgenic mice only. Taken together these data indicate the build-up and progressive accumulation of h-α-Syn aggregates in cortical somata and processes, but in nerve endings only in the striatum.

3.5. Late decline of striatal DA release in L62 mice is independent of cell loss in substantia nigra

Concomitant with the absence of h-α-Syn aggregates in dopaminergic neurones of the SNpC (Fig. 6A) we did not observe quantitative changes in any of the dopaminergic markers at 6–8 months of age (TH, pS40-TH, DAT and VMAT2, Fig. 8A–E).

In vivo brain dialysis confirmed that basal extracellular levels of DA were unchanged in transgenic mice at 3 and 9 months of age (Fig. 9A and B, left panels). However, the release of DA and turnover rates of its metabolites DOPAC and HVA were significantly reduced in 9 months old transgenic mice after challenge with amphetamine (Fig. 9B, right panel; genotype, time and interaction: F values > 2.3; p values ≤ 0.03; and Supplementary Fig. 2B and D), but there was no difference in response to amphetamine in younger mice (see Fig. 9A right panel and Supplementary Fig. 2A and C). To confirm this result in a behavioural

paradigm, WT and L62 mice were challenged with 2 mg/kg amphetamine at 3 and 6 months of age and their locomotor activity recorded in the open field. At the age of 3 months, amphetamine significantly increased the activity in WT and L62 mice (Fig. 9C; overall effect of genotype and interaction, F values > 4.4; p values < 0.0001). As found earlier, activity in the L62 saline cohort was lower than in WT saline (F1,85) = 5.8; p = 0.028) and amphetamine-induced heightening of activity was stronger in L62 (effect of treatment and interaction F values > 3.4; p values ≤ 0.03). At 6 months (Fig. 9D), there was an overall significant effect of genotype/treatment (F(3,174) = 104; p < 0.0001), L62 were less active than controls (F(1,84) = 64; p < 0.0001) and both genotypes responded with an increase in activity to amphetamine injections (F values > 46; p values < 0.0001). In contrast to younger mice, however, the activity of WT under amphetamine was reliably higher than for L62 (F(1,90) = 61; p < 0.0001). This is in agreement with reduced extracellular DA levels measured in old L62 mice after amphetamine challenge (Fig. 9B).

Collectively, these results suggest a progressive change in striatal dopaminergic neurotransmission over time in L62.

3.6. Altered dopaminergic receptor function precedes dopamine release deficit in L62 mice

Since the hypersensitive response to amphetamine in younger L62 mice cannot be explained by altered DA release/reuptake (Fig. 9A), we explored the possibility of alterations in dopamine receptor function. Increased levels of dopamine may be more efficient if the levels or sensitivity of D1/D2 receptors are differentially changed as a corollary of h-α-Syn expression in glutamatergic terminals of the striatum.

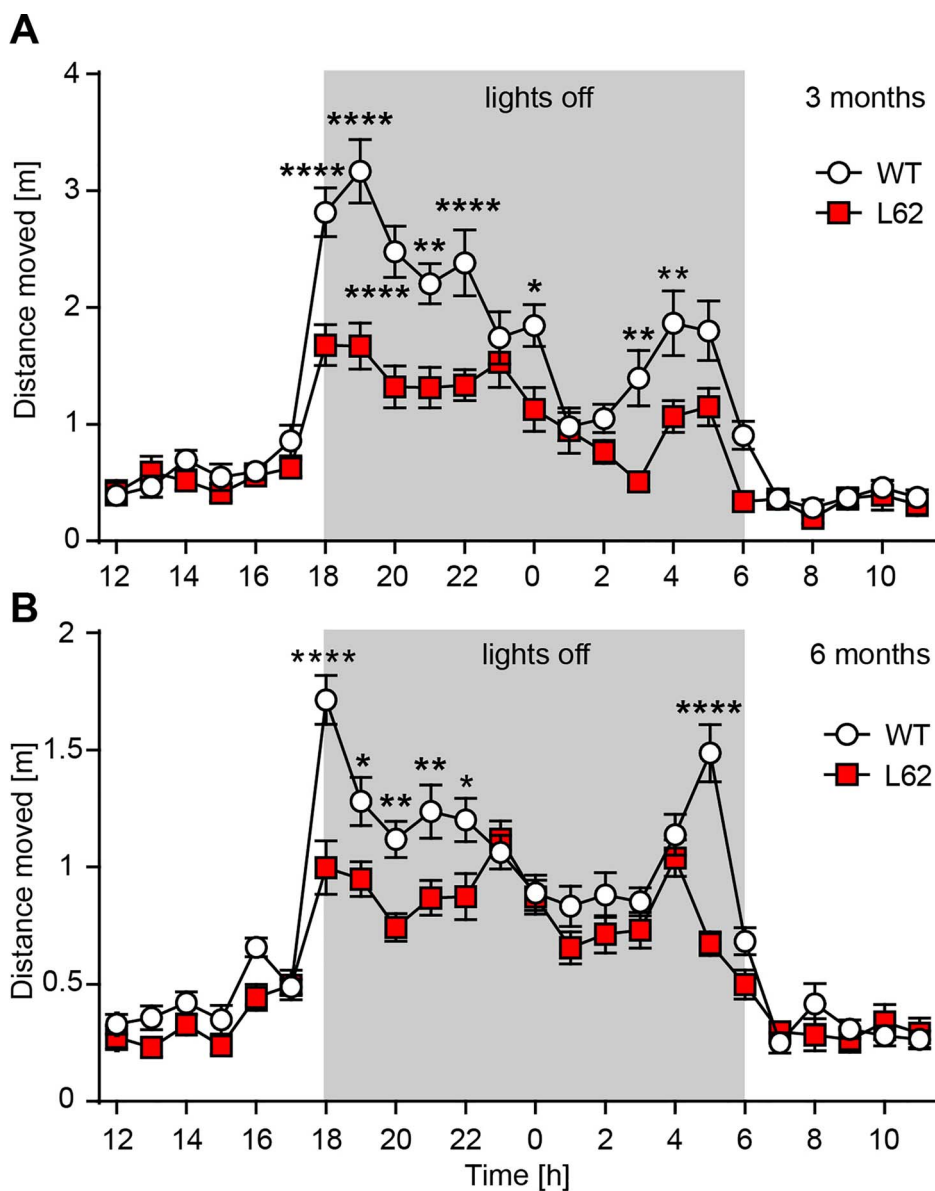**Fig. 5.** Reduced motor activity in L62 persists in a social environment and is not driven by anxiety. Activity monitoring of group-housed male mice in the home cage revealed that L62 mice are significantly less active than WT during the active phase (lights off) at 3 months (A) and 6 months (B) of age. (C–F) Anxiety behaviour of 6 months old male mice showed no genotype related differences for L62 mice and WT litters during the elevated plus maze testing. Values are given as mean ± S.E in hourly bins as time of day. Bonferroni post-test: *: $p < 0.05$, **: $p < 0.01$ and ****: $p < 0.0001$ vs. WT.

Consequently, we systemically administered the D1 receptor agonist SKF81297 and the D2 receptor agonist quinpirole prior to locomotor testing in the open field of L62 and WT mice, aged 3 months.

Mice of both genotypes injected with a high dose (5 mg/kg) of SKF81297 showed an overall significant increase of ambulation compared to saline-treated animals during the course of a 60-min trial (saline vs. 5 mg/kg; Fig. 10A for WT $F_{(1,14)} = 9.94$, $p = 0.007$ and Fig. 10B for L62 $F_{(1,12)} = 31.75$, $p = 0.0001$). Intriguingly, an effect
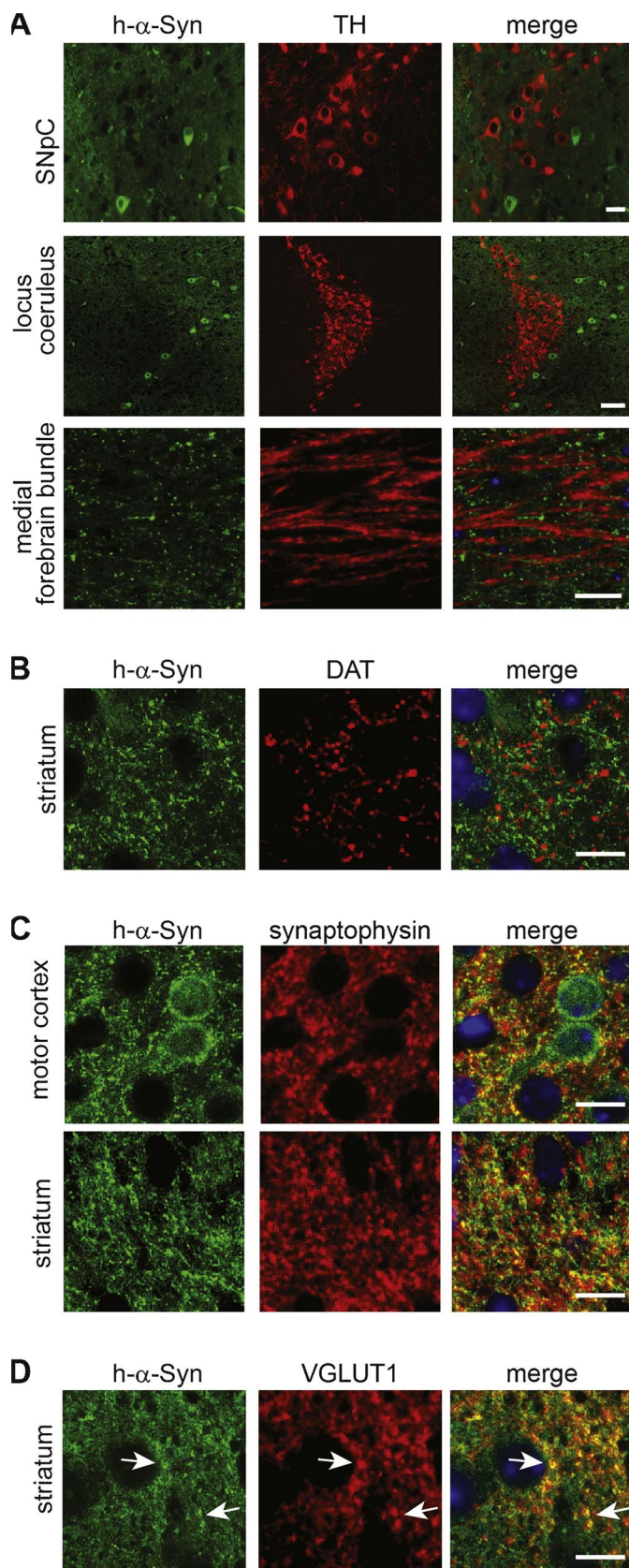
Fig. 6. Glutamatergic but not dopaminergic neurones are affected by h-α-Syn inclusions in L62 mice. (A) h-α-Syn inclusions (green) are absent from TH-positive neurones (red) of the SNpC and the locus coeruleus, as well as from nigrostriatal projections of the medial forebrain bundle, as shown by double label immunofluorescence of L62 midbrain sections. (B) Accordingly, DAT-positive synaptic terminals (red) in the striatum did not co-localise with the transgene (green: h-α-Syn). (C) Co-localisation of α-syn and the synaptic marker synaptophysin confirms the presynaptic accumulation of α-syn in cortical and striatal synapses; the presynaptic co-localisation of both proteins is seen as yellow puncta in the merged images. (D) In the striatum presynaptic α-syn is expressed in glutamatergic synapses, shown by co-staining with the glutamatergic marker VGLUT1 (yellow puncta). Scale bars: (A) 15 μm for SNpC, 50 μm for locus coeruleus and 50 μm for medial forebrain bundle, (B–D) 20 μm. (For interpretation of the references to color in this figure legend, the reader is referred to the web version of this article.)

defined as movement at a speed of > 25 cm/s, but spent significantly less time resting after injection of SKF81297 (Fig. 10C and D; main effect of treatment: C and D: F values $(2,38) > 14.76$, p values < 0.0001). Again, only L62 mice receiving a low dose of SKF81297 were significantly more active than saline-treated mice (Bonferroni's post-test: $p < 0.05$).

Low doses of quinpirole activate presynaptic D2 autoreceptors and induce suppression of motor activity by reducing dopamine release [38]. Accordingly, injection of 0.025 mg/kg quinpirole induced a decrease in activity in both genotypes (Fig. 10E; main effect of genotype/treatment $F(3,25) = 12.04$; $p < 0.0001$ and interaction $F(15,125) = 2.92$; $p < 0.0005$). The genotype effect seen in saline-treated animals during a 30-min trial was abolished in quinpirole-treated subjects (genotype effect saline: $F(1,12) = 4.77$; $p = 0.049$; quinpirole: ns), but the time course of the inhibition was different in WT compared to L62 (interaction $F(5,65) = 2.85$; $p = 0.022$). Furthermore, suppression of activity by quinpirole, measured as immobility, was increased in both WT and L62 to a similar extent (Fig. 10F; effect of treatment $F(1,25) = 31.31$; $p < 0.0001$; see asterisks for Bonferroni's post-test). Hence it appears that L62 mice differ considerably from WT in their sensitivity to dopaminergic receptor agonists acting through D1 receptors. By contrast, responses to D2 agonists appear far less compromised. Thus, the behavioural sensitisation to amphetamine could be caused by a disproportion between D1/D2 receptor levels due to accumulation of h-α-Syn in striatal glutamatergic terminals.

4. Discussion

Transgenic mice reported here show that overexpression of human α-Syn is sufficient to induce formation of α-Syn inclusions in neurones through self-aggregation as has been reported by others [20,22,39]. Such inclusions were absent from dopaminergic neurones in our models. Since α-Syn was identified in cortical cell bodies and processes, as well as in striatal terminals, we conclude that overexpression of h-α-Syn induced modulation of non-dopaminergic neurotransmission in fronto-striatal circuitry and that this is sufficient to change dopamine release and induce bradykinesia, independent of Lewy body pathology in SNpC. We were unable to obtain mice expressing truncated forms of h-α-Syn protein (data not shown). Such truncated forms of h-α-Syn can, however, induce aggregation *in vitro* [40] and *in vivo* when expressed in dopaminergic neurones [41]. Mutations in the h-α-Syn gene, e.g. the A53T or the A30P mutations, are not required to induce self-aggregation of the protein and it has been shown that such mutations only enhance development and progression of α-Syn pathology [20,42]. In humans, such mutations are associated with familiar PD, which account for 10% of clinical PD cases only. Given the high prevalence of sporadic PD [43], the overexpression of wild-type h-α-Syn is therefore a more physiologically relevant means to mimic the clinical appearance of PD [23] and our discussion here is focussed on a comparison of our mouse lines with existing transgenic lines [44,45].

Heterogeneity about regional h-α-Syn may arise from the use of different promotors of the transgene, which may exert variation in regional expression. Others have confirmed the utility of the *Thy1*

of a low dose (0.5 mg/kg) of SKF81297 was only seen in L62 ($F(1,11) = 8.82$; $p = 0.013$), but not WT control mice. Similarly, mice of both genotypes showed more attempts to initiate high activity, which is
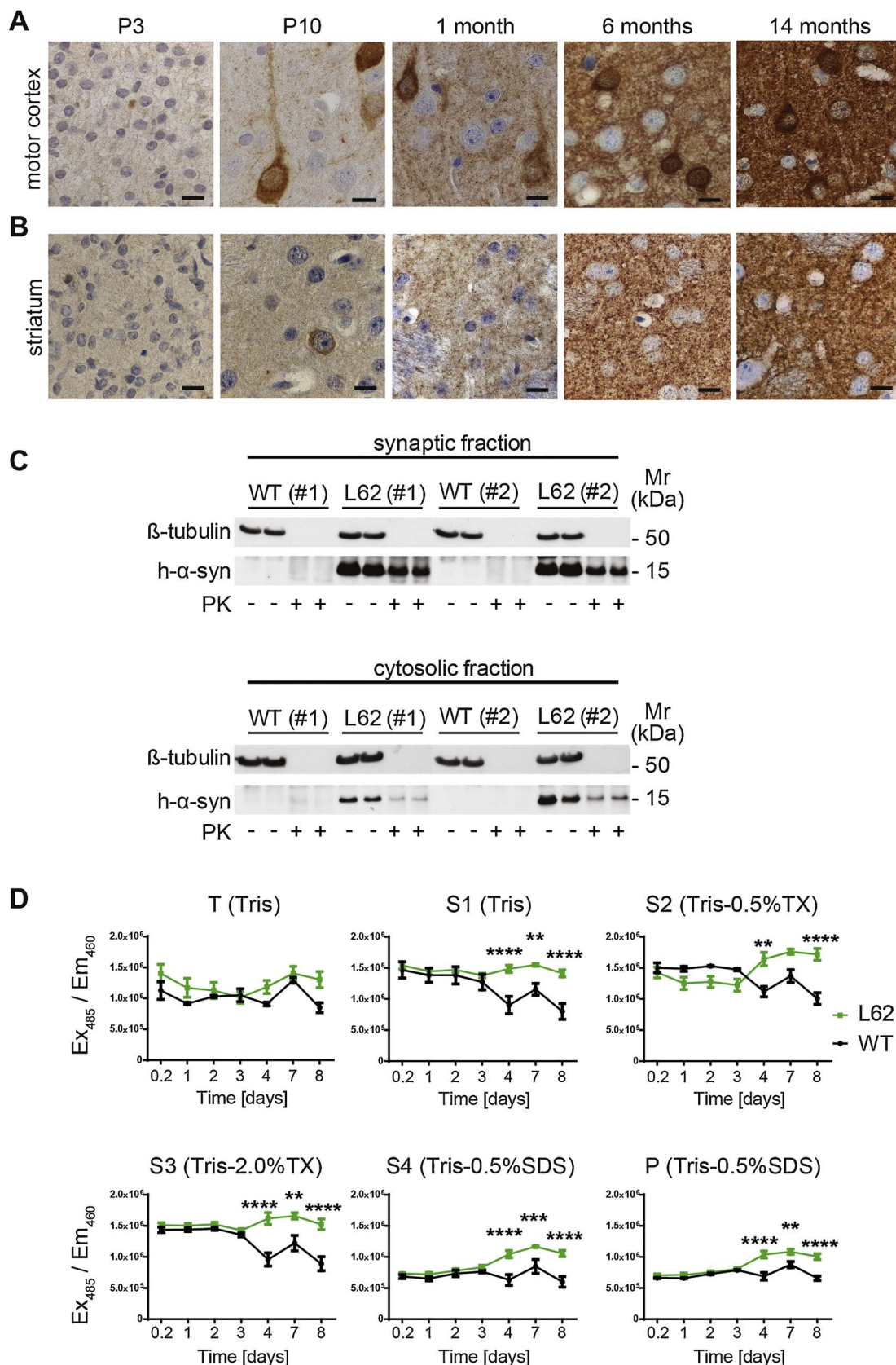
Fig. 7. h-α-Syn accumulates with increased age and forms aggregates, which bind thioflavin and are PK-resistent. (A) Immunohistology of L62 brain sections with the antibody mAb 204 in motor cortex (A) and striatal sections (B) indicates an age dependent increase in h-α-syn staining intensity. (C) h-α-Syn is more abundant in synaptic than in cytosolic fractions and is resistant to cleavage with PK, while ß-tubulin is not. (D) Thioflavin-binding of sequentially extracted proteins from the cortex revealed h-α-Syn to accumulate over time, measured as higher thioflavin emission in L62 mice compared to WT litters, aged 4 months. **: $p < 0.01$ and ****: $p < 0.0001$ vs. WT.
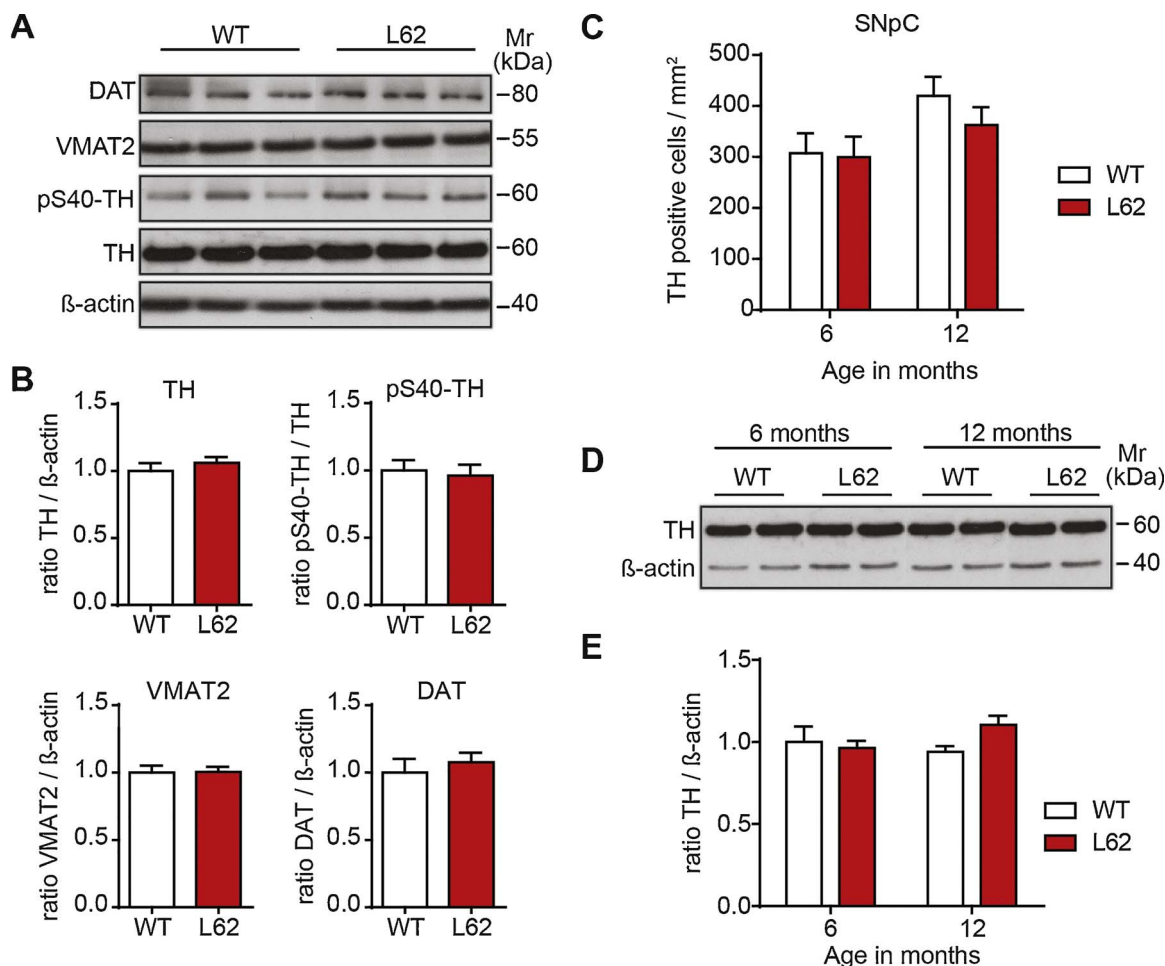
Fig. 8. L62 mice express normal levels of dopaminergic protein markers. (A) SDS-PAGE and semidry immunoblotting for TH, pSer40-TH, DAT and VMAT2 were conducted with 6–8 months old midbrain specimen. (B) Densitometry revealed similar expression levels of these synaptic markers between genotypes. (C) Manual counting of TH-positive neurones in SNpC (Bregma −3.80 ± 0.25 mm) and (D and E) immunoblot analysis of midbrain lysates at different ages revealed similar numbers of dopaminergic neurones in L62 and WT at 6 and 12 months of age.

promotor in h-α-Syn models of PD. Importantly, a ten-fold increase in h-α-Syn over endogenous synuclein levels caused reliable and persistent pathology and behavioural dysfunction in young mice [22,46]. Our three mouse models confirm the requirement of a higher number of cells expressing h-α-Syn for the early emergence of endophenotypes of PD. Despite similar gene expression profiles, the number of cells affected by h-α-Syn pathology was indicative of behavioural outcome. There was a progressive increase in the number of h-α-Syn-containing cells during ageing of L56, whereas the number of affected cells was maximal already at 3 months in both L58 and L62 mice. Since such differences in pathology are not explained by variations in gene expression, it is likely that gene insertion and cell-related expression are leading to these differences [47]. Nevertheless, pharmacological and behavioural phenotypes were also age-related in these lines.

In L56 and L58 only few cortical motor neurones stained for h-α-Syn inclusions, whereas prominent inclusions were detected in cortical and spinal motor neurones in L62 and we found that the level of h-α-Syn pathology determined the severity of the observed bradykinesia. L56 displayed a late onset, mild motor phenotype. By contrast, L62 mice with dense h-α-Syn aggregation in e.g. cortical motor neurones showed early onset motor deficits in open field, RotaRod, balance beam, CatWalk and activity monitoring. These phenotypes occurred despite the lack of significant dopaminergic alterations or the accumulation of h-α-Syn in TH-positive neurones in the substantia nigra. This contrasts with the line 61 model of the Chesselet group, which presents with hyperactivity in the open field due to increased striatal DA [23], but

which also lacks synuclein expression in the SNpC.

The overall pathology of cortical, brain stem and spinal neurones in our model is consistent with observations of van der Putten and colleagues [20] as well as Delenclos and co-workers [48], where these authors reported no or very low expression of *Thy1*-driven wild-type h-α-Syn in the SNpC but severe cortical and spinal motor neurone pathology [20]. In contrast, Rockenstein and colleagues reported accumulation of *Thy1*-driven h-α-Syn in the SN and other subcortical nuclei but not in the spinal cord of their line 61 model [22]. These latter authors did not differentiate between SNpC and SNpR precluding a direct comparison with more recent investigations of *Thy1*-directed α-Syn models. We consider it likely that the discrepancy for α-Syn expression and accumulation pattern for these *Thy1*-driven wild-type h-α-Syn models arises from the use of different expression cassettes, different sites of transgene integration or subtle differences in the antibodies and protocols used.

None of the mouse lines described here accumulated h-α-Syn in neurones of the SNpC. Moreover, synaptic markers for dopaminergic cells in the striatum were normal in mice aged 6 months. This is consistent with other *Thy1* models overexpressing wild-type h-α-Syn [22]. Although the onset of the activity of the *Thy1* promotor is not clearly defined, we and others have been unable to detect loss of TH-positive cells even at the age of > 12 months [22]. Yet, a progressive lowering of amphetamine-induced dopamine release in striatum appeared in L62 between 3 and 9 months of age suggesting functional changes within SNpC possibly due to expression of h-α-Syn at levels below the
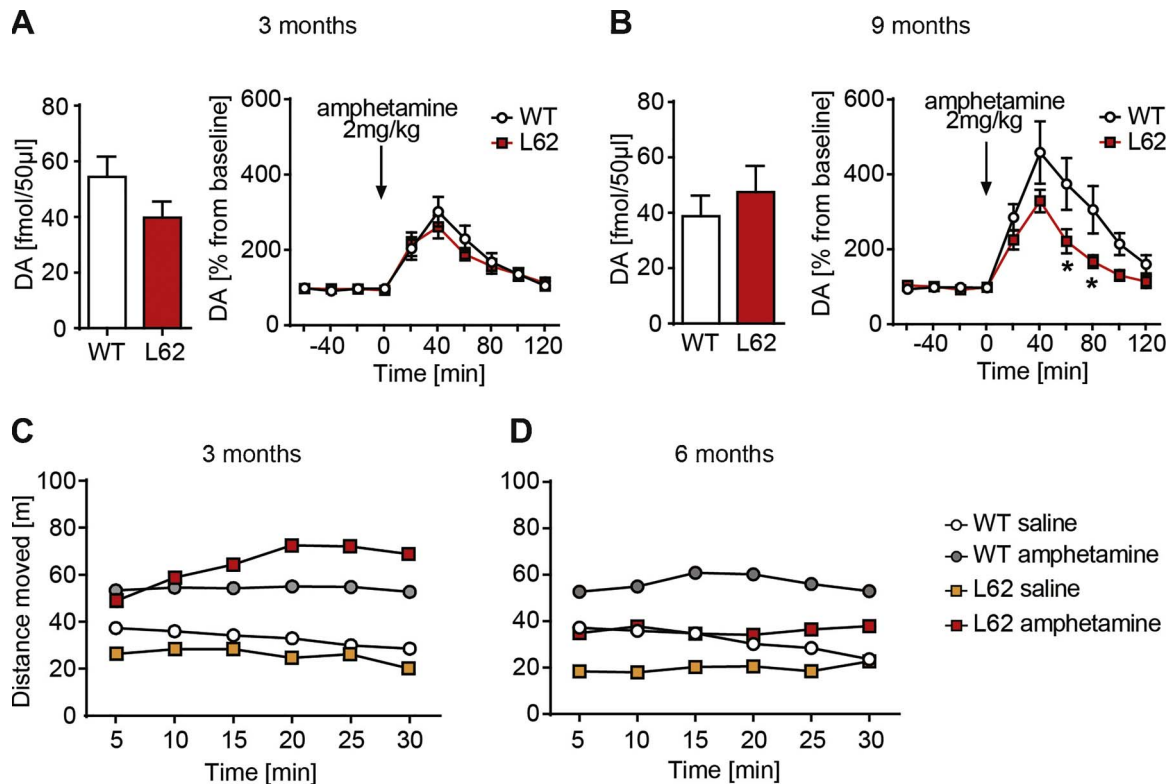
Fig. 9. L62 mice show a progressive decline of DA release. (A and B) DA measurements using in vivo brain dialysis performed in dorsal striatum of male WT and L62 mice. (A) At 3 months of age basal DA (left) and DA release following amphetamine administration (2 mg/kg: right) in L62 mice did not differ from WT. (B) At the age of 9 months, L62 mice displayed lower DA release following amphetamine challenge, while basal DA levels remained unchanged. (C and D) Mice were given a single i.p. injection of 2 mg/kg amphetamine or 0.9% saline and immediately placed in the open field arena after injection and ambulation measured for 30 min. Three months old WT and L62 mice walked significantly more in response to amphetamine compared to saline and locomotor sensitization was significantly higher in transgenic L62 mice (C). The response to amphetamine of L62 mice was less pronounced compared to WT at 6 months of age and L62 mice showed significantly less sensitization to amphetamine (D). Values are given as mean (S.E. omitted for clarity). *: $p < 0.05$.

detection threshold of our antibodies. This idea is further supported by the reduced reaction to amphetamine in 6-month old animals (Fig. 9) and is consistent with a lack of amphetamine-induced stereotypies in other *Thy1* α-Syn mice [49]. It also confirms that an overall lowering of dopamine release under behavioural or pharmacological challenges can be observed in the absence of α-Syn inclusions in striatal input structures of dopaminergic origin in h-α-Syn mice. Finally, the lack of α-Syn inclusions in TH-positive SNpC neurones was not correlated with the magnitude of striatal dysfunction in response to pharmacological treatment. This is in agreement with paraquat intoxication enhancing the number of proteinase-K-resistant α-Syn aggregates in the substantia nigra, while not worsening the behavioural deficits in these *Thy1* h-α-Syn mice [50].

Nevertheless, the *Thy1* promotor is capable of driving h-α-Syn expression in TH-positive cells of the substantia nigra. This has been confirmed using h-α-Syn containing the A53T mutation of familial forms of PD [20]. These mice did develop ubiquitin-positive inclusions in neurones suggesting Lewy body like α-Syn aggregates. Nevertheless, it should be noted that such cases model a small number of PD patients and not the overwhelming majority of idiopathic forms. That a strong expression of wild-type h-α-Syn can be achieved in nigral TH-positive cells using promotors for prion protein [21] or TH suggests that *Thy1* is specifically targeting non-dopaminergic pathways and our mouse model therefore represents a slow onset form of synucleinopathy with PD-like symptoms. It is reminiscent to the first α-Syn mouse developed by Masliah and co-workers [39] using the platelet-derived growth factor β promotor, which also did not lead to h-α-Syn expression in SNpC. Striatal dopamine levels, however, were lowered in mice older than 12 months of age [51], and this is in agreement with our observation in L62 mice that functional changes in the nigro-striatal system can be achieved by low h-α-Syn expression in mice leading to behavioural impairments.

It therefore appears that changes in dopamine release and dopamine receptor sensitivity are driven by the predominant expression of h-α-Syn in glutamatergic neurones of the cortex (and possibly thalamus − not confirmed). Such endophenotypes of wild type h-α-Syn mice represent a state of pre-manifest PD [52,53], in which presynaptic mobilisation of the reserve pool of neurotransmitter vesicles is compromised [54,55]. α-Syn plays a critical role in this process as it is located pre-synaptically and acts as a molecular chaperone interacting with SNARE proteins to aid transmitter release and vesicle recycling [56]. These actions appear to be compromised by the A30P mutation in the synuclein gene and are not specific for dopaminergic synapses. For example, h-α-Syn mice expressing the transgene controlled by the human α-Syn regulatory element presented with normal evoked mossy fibre field EPSP (excitatory post-synaptic potential) slopes until a stimulation current of 200 μA, above which there was a 20% lowering of the EPSP [54]. Slices from these animals were also impaired in synaptic plasticity (paired pulse facilitation; frequency facilitation) suggesting that overexpression of h-α-Syn in glutamatergic neurones may lead to a pre-manifest PD. Knock-out of murine α-Syn had the opposite effect, hyperexcitability but also reduced plasticity. These results have been recently confirmed for medium spiny neurones in the striatum of h-α-Syn mice under control of Thy1 promotor [57]. Whole cell patch clamp recordings from spiny neurones in the dorsolateral striatum confirmed significantly reduced spontaneous EPSCs in hemispheric sections from h-α-Syn from 35 days of age onwards. Moreover, there was a 40% lowering of evoked EPSCs in all stimulation intensities (0.3–1 mA) and a similar reduction in N-methyl-D-aspartate (NMDA) receptor mediated currents in h-α-Syn tissue [57]. These adaptations at cortico-striatal synapses appear to occur prior to dopamine depletion and lead to subtle preclinical phenotypes. Our L62 mice appear to reflect similar
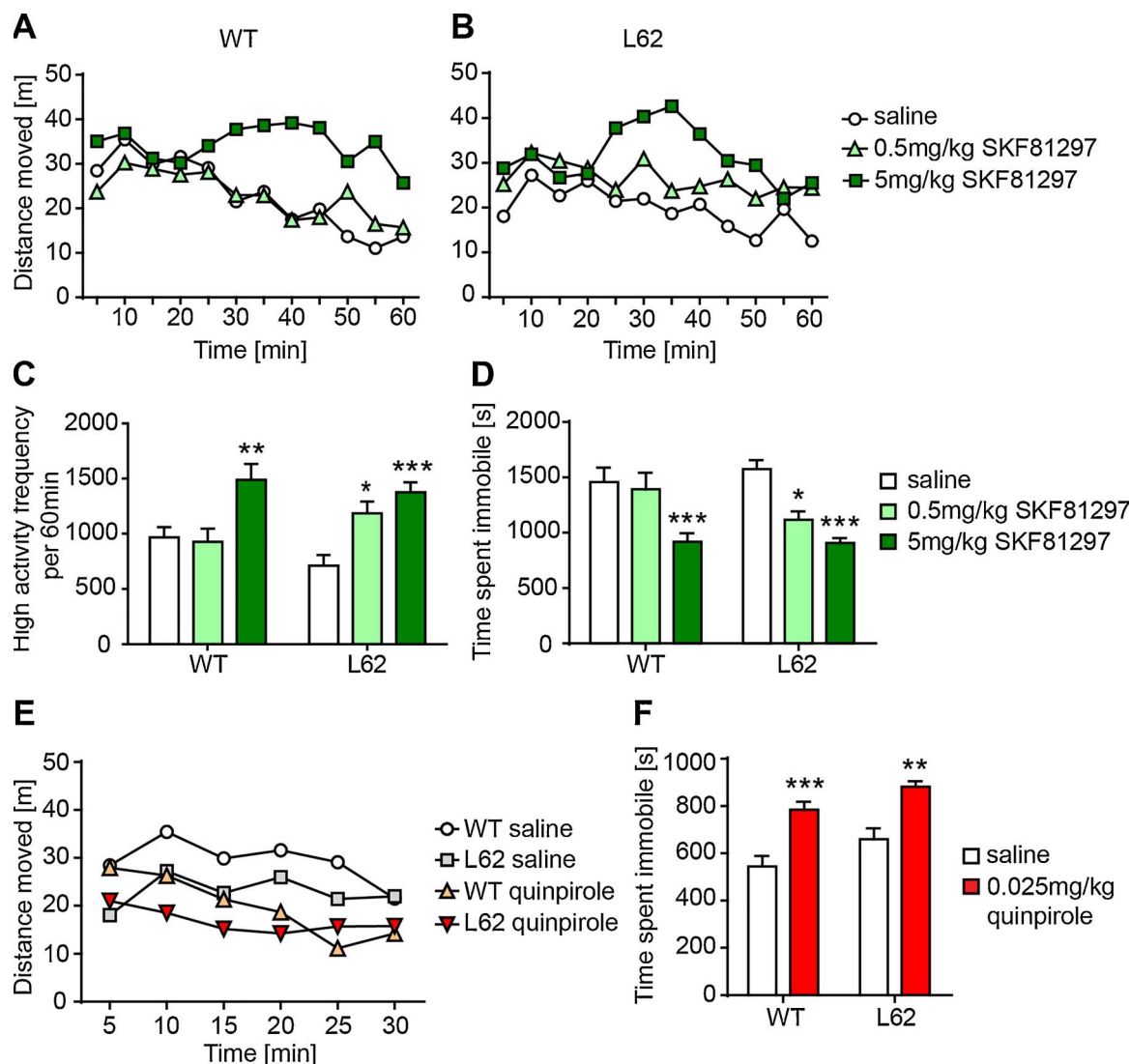
Fig. 10. Sensitization of D1 but not D2 pathways in L62 mice. (A-F) Locomotor activity of 3 months old WT and L62 male mice recorded in the open field following acute injection of specific D1 and D2 receptor agonists SKF81297 and quinpirole, respectively. Treatment with 5 but not 0.5 mg/kg SKF81297 increased locomotion in WT mice during a 60 min trial (A). In contrast, L62 mice walked significantly more after treatment with 0.5 and 5 mg/kg SKF81297 relative to saline (B). L62 but not WT mice showed significantly more attempts to initiate fast movements (> 25 cm/s) (C) and spent less time resting (< 2 cm/s) (D) in the 60 min period following administration of 0.5 mg/kg SKF81297 (Bonferroni's post-test compared to vehicle: *p < 0.05, **p < 0.01 and ***p < 0.001). (E-F) The effect of 0.025 mg/kg quinpirole was tested for 30 min in the open field. A significant suppression of locomotion (E) and an increase of resting time (F) were found in both genotypes. Values are given as mean (S.E. omitted for clarity).

prodromal manifestations at 3 months of age when there is little evidence for dopaminergic alterations at baseline or at challenge (Fig. 9), but a progressive phenotype at 6–9 months of age when severe dopamine depletion symptoms occur. The reduction in glutamatergic release was coincident with hypersensitivity of post-synaptic D1, but not presynaptic D2 receptors, thereby explaining the strong hyperactivity in L62 mice. The clinical relevance and cellular mechanism for this clinically relevant finding, however, requires further examination.

5. Conclusions

Collectively, we have shown that overexpression of h-α-Syn under the *Thy1* regulatory element promotes expression of h-α-Syn in multiple neuronal subpopulations. Intriguingly, this did not include TH-positive dopaminergic neurones, but glutamate containing principle cells in the cortex with direct synaptic contacts to medium spiny neurons of the striatum. Loading of glutamatergic cell bodies and processes with h-α-Syn typically leads to a lowering in vesicular release and constitutes a state of pre-manifest PD. Such a glutamatergic phenotype appears to influence behaviours modulated by dopamine and after further ageing

leads to more severe hypodopaminergic parkinsonian manifestations. This time course offers a novel means for understanding the principle mechanisms and putative treatment options for PD.

Author contribution

SF, KS, VM, DH, JER, FT designed and performed experiments; PF and MS performed microdialysis experiments; KS, SF and GR performed statistical analyses; KS, SF, GR, CRH, CMW and FT conceived the project; KS, SF, GR, CRH, CMW and FT wrote the paper and all authors reviewed the final manuscript.

Conflict of interest

None.

behavioural testing and maintenance of animals. This work was funded by TauRx Therapeutics Ltd., Singapore. C.R.H. and C.M.W. declare that they are officers in TauRx Therapeutics Ltd.

Appendix A. Supplementary data

Supplementary data associated with this article can be found, in the online version, at https://doi.org/10.1016/j.bbr.2017.11.025.

References

[1] C. Hansen, T. Bjorklund, G.H. Petit, M. Lundblad, R.P. Murmu, P. Brundin, J.Y. Li, A novel alpha-synuclein-GFP mouse model displays progressive motor impairment, olfactory dysfunction and accumulation of alpha-synuclein-GFP, Neurobiol. Dis. 56 (2013) 145–155.

[2] C.M. Tolleson, J.Y. Fang, Advances in the mechanisms of Parkinson's disease, Discov. Med. 15 (2013) 61–66.

[3] P. Bargiotas, S. Konitsiotis, Levodopa-induced dyskinesias in Parkinson's disease: emerging treatments, Neuropsychiatr. Dis. Treat. 9 (2013) 1605–1617.

[4] S. George, N.L. Rey, N. Reichenbach, J.A. Steiner, P. Brundin, Alpha-synuclein: the long distance runner, Brain Pathol. 23 (2013) 350–357.

[5] M.C. Chartier-Harlin, J. Kachergus, C. Roumier, V. Mouroux, X. Douay, S. Lincoln, C. Levecque, L. Larvor, J. Andrieux, M. Hulihan, N. Waucquier, L. Defebvre, P. Amouyel, M. Farrer, A. Destee, Alpha-synuclein locus duplication as a cause of familial Parkinson's disease, Lancet 364 (2004) 1167–1169.

[6] R. Kruger, W. Kuhn, T. Muller, D. Woitalla, M. Graeber, S. Kosel, H. Przuntek, J.T. Epplen, L. Schols, O. Riess, Ala30Pro mutation in the gene encoding alpha-synuclein in Parkinson's disease, Nat. Genet. 18 (1998) 106–108.

[7] D.M. Maraganore, M. de Andrade, T.G. Lesnick, K.J. Strain, M.J. Farrer, W.A. Rocca, P.V. Pant, K.A. Frazer, D.R. Cox, D.G. Ballinger, High-resolution whole-genome association study of Parkinson disease, Am. J. Hum. Genet. 77 (2005) 685–693.

[8] I. Ubeda-Banon, D. Saiz-Sanchez, C. de la Rosa-Prieto, A. Martinez-Marcos, alpha-Synuclein in the olfactory system in Parkinson's disease: role of neural connections on spreading pathology, Brain Struct. Funct. 219 (2014) 1513–1526.

[9] J.A. Obeso, M.C. Rodriguez-Oroz, M. Rodriguez, J.L. Lanciego, J. Artieda, N. Gonzalo, C.W. Olanow, Pathophysiology of the basal ganglia in Parkinson's disease, Trends Neurosci. 23 (2000) S8–19.

[10] K.J. Doorn, A. Goudriaan, C. Blits-Huizinga, J.G. Bol, A.J. Rozemuller, P.V. Hoogland, P.J. Lucassen, B. Drukarch, W.D. van de Berg, A.M. van Dam, Increased amoeboid microglial density in the olfactory bulb of Parkinson's and Alzheimer's patients, Brain Pathol. 24 (2014) 152–165.

[11] A. Maass, H. Reichmann, Sleep and non-motor symptoms in Parkinson's disease, J. Neural Transm. (Vienna) 120 (2013) 565–569.

[12] K.L. Parker, D. Lamichhane, M.S. Caetano, N.S. Narayanan, Executive dysfunction in Parkinson's disease and timing deficits, Front. Integr. Neurosci. 7 (2013) 75.

[13] S. Ltic, M. Perovic, A. Mladenovic, N. Raicevic, S. Ruzdijic, L. Rakic, S. Kanazir, Alpha-synuclein is expressed in different tissues during human fetal development, J. Mol. Neurosci. 22 (2004) 199–204.

[14] D.C. DeWitt, E. Rhoades, Alpha-synuclein can inhibit SNARE-mediated vesicle fusion through direct interactions with lipid bilayers, Biochemistry 52 (2013) 2385–2387.

[15] S.E. Eisbach, T.F. Outeiro, Alpha-synuclein and intracellular trafficking: impact on the spreading of Parkinson's disease pathology, J. Mol. Med. (Berl.) 91 (2013) 693–703.

[16] O.W. Wan, K.K. Chung, The role of alpha-synuclein oligomerization and aggregation in cellular and animal models of Parkinson's disease, PLoS One 7 (2012) e38545.

[17] A.H. Schapira, E. Bezard, J. Brotchie, F. Calon, G.L. Collingridge, B. Ferger, B. Hengerer, E. Hirsch, P. Jenner, N.N. Le, J.A. Obeso, M.A. Schwarzschild, U. Spampinato, G. Davidai, Novel pharmacological targets for the treatment of Parkinson's disease, Nat. Rev. Drug Discov. 5 (2006) 845–854.

[18] L.V. Kalia, J.M. Brotchie, S.H. Fox, Novel nondopaminergic targets for motor features of Parkinson's disease: review of recent trials, Mov. Disord. 28 (2013) 131–144.

[19] A. Wilkaniec, J.B. Strosznajder, A. Adamczyk, Toxicity of extracellular secreted alpha-synuclein: its role in nitrosative stress and neurodegeneration, Neurochem. Int. 62 (2013) 776–783.

[20] H. van der Putten, K.H. Wiederhold, A. Probst, S. Barbieri, C. Mistl, S. Danner, S. Kauffmann, K. Hofele, W.P. Spooren, M.A. Ruegg, S. Lin, P. Caroni, B. Sommer, M. Tolnay, G. Bilbe, Neuropathology in mice expressing human alpha-synuclein, J. Neurosci. 20 (2000) 6021–6029.

[21] B.I. Giasson, J.E. Duda, S.M. Quinn, B. Zhang, J.Q. Trojanowski, V.M. Lee, Neuronal alpha-synucleinopathy with severe movement disorder in mice expressing A53T human alpha-synuclein, Neuron 34 (2002) 521–533.

[22] E. Rockenstein, M. Mallory, M. Hashimoto, D. Song, C.W. Shults, I. Lang, E. Masliah, Differential neuropathological alterations in transgenic mice expressing alpha-synuclein from the platelet-derived growth factor and Thy-1 promoters, J. Neurosci. Res. 68 (2002) 568–578.

[23] M.F. Chesselet, F. Richter, C. Zhu, I. Magen, M.B. Watson, S.R. Subramaniam, A progressive mouse model of Parkinson's disease: the Thy1-aSyn (Line 61) mice, Neurotherapeutics 9 (2012) 297–314.

[24] A. Pisani, G. Bernardi, J. Ding, D.J. Surmeier, Re-emergence of striatal cholinergic interneurons in movement disorders, Trends Neurosci. 30 (2007) 545–553.

[25] D.B. Lester, T.D. Rogers, C.D. Blaha, Acetylcholine-dopamine interactions in the pathophysiology and treatment of CNS disorders, CNS Neurosci. Ther. 16 (2010) 137–162.

[26] G.E. Alexander, M.D. Crutcher, Functional architecture of basal ganglia circuits: neural substrates of parallel processing, Trends Neurosci. 13 (1990) 266–271.

[27] P. Calabresi, B. Picconi, A. Tozzi, V. Ghiglieri, F.M. Di, Direct and indirect pathways of basal ganglia: a critical reappraisal, Nat. Neurosci. 17 (2014) 1022–1030.

[28] M. Day, Z. Wang, J. Ding, X. An, C.A. Ingham, A.F. Shering, D. Wokosin, E. Ilijic, Z. Sun, A.R. Sampson, E. Mugnaini, A.Y. Deutch, S.R. Sesack, G.W. Arbuthnott, D.J. Surmeier, Selective elimination of glutamatergic synapses on striatopallidal neurons in Parkinson disease models, Nat. Neurosci. 9 (2006) 251–259.

[29] H. Bergman, T. Wichmann, M.R. DeLong, Reversal of experimental parkinsonism by lesions of the subthalamic nucleus, Science 249 (1990) 1436–1438.

[30] P. Calabresi, B. Picconi, L. Parnetti, F.M. Di, A convergent model for cognitive dysfunctions in Parkinson's disease: the critical dopamine-acetylcholine synaptic balance, Lancet Neurol. 5 (2006) 974–983.

[31] H. Schagger, Tricine-SDS-PAGE, Nat. Protoc. 1 (2006) 16–22.

[32] Franklin, Paxinos, The Mouse Brain in Stereotaxic Coordinates, Compact, 3rd edn., Academic Press, New York, 2008.

[33] P. Fadda, M. Scherma, A. Fresu, M. Collu, W. Fratta, Dopamine and serotonin release in dorsal striatum and nucleus accumbens is differentially modulated by morphine in DBA/2J and C57BL/6J mice, Synapse 56 (2005) 29–38.

[34] E.I. Kyriakou, J.G. van der Kieft, R.C. de Heer, A. Spink, H.P. Nguyen, J.R. Homberg, J.E. van der Harst, Automated quantitative analysis to assess motor function in different rat models of impaired coordination and ataxia, J. Neurosci. Methods 268 (2016) 171–181.

[35] V. Melis, C. Zabke, K. Stamer, M. Magbagbeolu, K. Schwab, P. Marschall, R.W. Veh, S. Bachmann, S. Deiana, P.H. Moreau, K. Davidson, K.A. Harrington, J.E. Rickard, D. Horsley, R. Garman, M. Mazurkiewicz, G. Niewiadomska, C.M. Wischik, C.R. Harrington, G. Riedel, F. Theuring, Different pathways of molecular pathophysiology underlie cognitive and motor tauopathy phenotypes in transgenic models for Alzheimer's disease and frontotemporal lobar degeneration, Cell. Mol. Life Sci. 72 (2015) 2199–2222.

[36] L. de Visser, R. van den Bos, B.M. Spruijt, Automated home cage observations as a tool to measure the effects of wheel running on cage floor locomotion, Behav. Brain Res. 160 (2005) 382–388.

[37] L. Robinson, A. Plano, S. Cobb, G. Riedel, Long-term home cage activity scans reveal lowered exploratory behaviour in symptomatic female Rett mice, Behav. Brain Res. 250 (2013) 148–156.

[38] A. Usiello, J.H. Baik, F. Rouge-Pont, R. Picetti, A. Dierich, M. LeMeur, P.V. Piazza, E. Borrelli, Distinct functions of the two isoforms of dopamine D2 receptors, Nature 408 (2000) 199–203.

[39] E. Masliah, E. Rockenstein, I. Veinbergs, M. Mallory, M. Hashimoto, A. Takeda, Y. Sagara, A. Sisk, L. Mucke, Dopaminergic loss and inclusion body formation in alpha-synuclein mice: implications for neurodegenerative disorders, Science 287 (2000) 1265–1269.

[40] C.W. Liu, B.I. Giasson, K.A. Lewis, V.M. Lee, G.N. DeMartino, P.J. Thomas, A precipitating role for truncated alpha-synuclein and the proteasome in alpha-synuclein aggregation—implications for pathogenesis of Parkinson disease, J. Biol. Chem. 280 (2005) 22670–22678.

[41] M. Wakamatsu, A. Ishii, S. Iwata, J. Sakagami, Y. Ukai, M. Ono, D. Kanbe, S.I. Muramatsu, K. Kobayashi, T. Iwatsubo, M. Yoshimotoa, Selective loss of nigral dopamine neurons induced by overexpression of truncated human alpha-synuclein in mice, Neurobiol. Aging 29 (2008) 574–585.

[42] P.J. Kahle, M. Neumann, L. Ozmen, V. Muller, H. Jacobsen, A. Schindzielorz, M. Okochi, U. Leimer, P.H. van der, A. Probst, E. Kremmer, H.A. Kretzschmar, C. Haass, Subcellular localization of wild-type and Parkinson's disease-associated mutant alpha −synuclein in human and transgenic mouse brain, J. Neurosci. 20 (2000) 6365–6373.

[43] M.J. Farrer, Genetics of Parkinson disease: paradigm shifts and future prospects, Nat. Rev. Genet. 7 (2006) 306–318.

[44] P.M. Antony, N.J. Diederich, R. Balling, Parkinson's disease mouse models in translational research, Mamm. Genome 22 (2011) 401–419.

[45] I. Magen, M.F. Chesselet, Genetic mouse models of Parkinson's disease the state of the art, Prog. Brain Res. 184 (2010) 53–87.

[46] J.B. Watson, A. Hatami, H. David, E. Masliah, K. Roberts, C.E. Evans, M.S. Levine, Alterations in corticostriatal synaptic plasticity in mice overexpressing human alpha-synuclein, Neuroscience 159 (2009) 501–513.

[47] M. Jasin, M.E. Moynahan, C. Richardson, Targeted transgenesis, Proc. Natl. Acad. Sci. U. S. A 93 (1996) 8804–8808.

[48] M. Delenclos, L. Carrascal, K. Jensen, M. Romero-Ramos, Immunolocalization of human alpha-synuclein in the Thy1-aSyn (Line 61) transgenic mouse line, Neuroscience 277 (2014) 647–664.

[49] S.M. Fleming, J. Salcedo, C.B. Hutson, E. Rockenstein, E. Masliah, M.S. Levine, M.F. Chesselet, Behavioral effects of dopaminergic agonists in transgenic mice overexpressing human wildtype alpha-synuclein, Neuroscience 142 (2006) 1245–1253.

[50] P.O. Fernagut, C.B. Hutson, S.M. Fleming, N.A. Tetreaut, J. Salcedo, E. Masliah, M.F. Chesselet, Behavioral and histopathological consequences of paraquat intoxication in mice: effects of alpha-synuclein over-expression, Synapse 61 (2007) 991–1001.

[51] M. Hashimoto, E. Rockenstein, E. Masliah, Transgenic models of alpha-synuclein pathology: past, present, and future, Ann. N. Y. Acad. Sci. 991 (2003) 171–188.

[52] S.M. Fleming, N.A. Tetreault, C.K. Mulligan, C.B. Hutson, E. Masliah, M.F. Chesselet, Olfactory deficits in mice overexpressing human wildtype alpha-

synuclein, Eur. J. Neurosci. 28 (2008) 247–256.

[53] L. Wang, S.M. Fleming, M.F. Chesselet, Y. Tache, Abnormal colonic motility in mice overexpressing human wild-type alpha-synuclein, Neuroreport 19 (2008) 873–876.

[54] I. Gureviciene, K. Gurevicius, H. Tanila, Role of alpha-synuclein in synaptic gluta-mate release, Neurobiol. Dis. 28 (2007) 83–89.

[55] L. Yavich, H. Tanila, S. Vepsalainen, P. Jakala, Role of alpha-synuclein in pre-synaptic dopamine recruitment, J. Neurosci. 24 (2004) 11165–11170.

[56] S. Chandra, G. Gallardo, R. Fernandez-Chacon, O.M. Schluter, T.C. Sudhof, Alpha-synuclein cooperates with CSPalpha in preventing neurodegeneration, Cell 123 (2005) 383–396.

[57] N. Wu, P.R. Joshi, C. Cepeda, E. Masliah, M.S. Levine, Alpha-synuclein over-expression in mice alters synaptic communication in the corticostriatal pathway, J. Neurosci. Res. 88 (2010) 1764–1776.